The feasibility of monitoring CO_2 from high-resolution infrared sounders

A. Chédin,[1] R. Saunders,[2] A. Hollingsworth,[2] N. Scott,[1] M. Matricardi,[2] J. Etcheto,[3] C. Clerbaux,[4] R. Armante,[1] and C. Crevoisier[1]

Received 31 October 2001; revised 30 September 2002; accepted 4 October 2002; published 28 January 2003.

[1] Satellite instruments specifically designed to monitor atmospheric carbon dioxide concentrations have not been flown to date but, high-resolution infrared sounders, being launched in the next few years, may offer the possibility of at least a basic carbon dioxide monitoring capability. This paper explores the sensitivity of this new generation of advanced infrared sounders to changing carbon dioxide concentrations and also compares this with uncertainties due to the atmospheric temperature, water vapor, and minor constituent concentrations using the current background errors in numerical weather prediction models as a baseline. The sensitivity results shown are computed for the Infrared Atmospheric Sounding Interferometer (IASI), which is due to fly on the European METOP platform from 2005. We show that although the carbon dioxide signal is below or at the instrument noise for IASI and that uncertainties in temperature and water vapor errors can dominate, a careful averaging of the retrieved carbon dioxide fields over areas of 500×500 km^2 and 2 weeks should be able to extract changes at the level of 1% or less in the total column carbon dioxide amount. We also show results of an information content study for the Atmospheric InfraRed Sounder, AIRS, data, which suggests 50 channels are adequate for inferring the tropospheric carbon dioxide amounts but that they are not sensitive to CO_2 changes in the boundary layer. *INDEX TERMS:* 0365 Atmospheric Composition and Structure: Troposphere—composition and chemistry; 1640 Global Change: Remote sensing; 0394 Atmospheric Composition and Structure: Instruments and techniques; 3360 Meteorology and Atmospheric Dynamics: Remote sensing; *KEYWORDS:* Retrieval of carbon dioxide, climate monitoring, AIRS, IASI, IMG

Citation: Chédin, A., R. Saunders, A. Hollingsworth, N. A. Scott, M. Matricardi, J. Etcheto, C. Clerbaux, R. Armante, and C. Crevoisier, The feasibility of monitoring CO_2 from high-resolution infrared sounders, *J. Geophys. Res.*, *108*(D2), 4064, doi:10.1029/2001JD001443, 2003.

1. Introduction

[2] The carbon cycle is one of the most complex planetary phenomena. While its main features have been identified, our present knowledge is inadequate either to detect the changes that (almost certainly) have already occurred due to human activities, or to predict the changes (likely to be considerably greater) that can be expected in the future. However, in order to recognise human impacts, and assess their significance, we need to address the major areas of uncertainty regarding the functioning of the natural system.

[3] Our current observing system has a significant gap as knowledge of the global carbon cycle is based on sparse sampling on land, at sea and in the atmosphere. For example, we currently reconstruct regional carbon budgets from approximately 100 points. As a consequence, we cannot yet measure the components of the global carbon cycle with sufficient accuracy to balance the budget. While it is known that human activities add 5–6 billion tons (10^9) of carbon each year to the atmosphere, the annual increase in atmospheric CO_2 is equivalent to 3 billion tons of carbon. It had been thought that the oceans absorbed the remainder. However, recent estimates leave at least 1 billion tons unaccounted for. Improvements in the confidence of such estimates, and in our understanding of the uptake mechanisms involved, are therefore urgently needed for reliable predictions of future increases in atmospheric CO_2.

[4] To address these issues, greater geographical and seasonal coverage of CO_2 measurements in the upper ocean and in the atmosphere is required, linked to studies of the relevant physical and biological processes. Satellite measurements of the distribution of global atmospheric CO_2 would in principle fill this gap in scale [*Rayner and O'Brien*, 2001]. Measurements that densely sample the atmosphere would provide a crucial constraint, allowing uncertainty in transport versus other information (on source and sink characteristics) to be separated and reduced. A proof of concept study can already be demonstrated with

[1]Laboratoire de Météorologie Dynamique, École Polytechnique, Palaiseau, France.
[2]European Centre for Medium-Range Weather Forecasting, Shinfield Park, Reading, UK.
[3]Laboratoire d'Océanographie Dynamique et de Climatologie, Université Pierre et Marie Curie, Paris, France.
[4]Service d'Aéronomie, Université de Paris, Paris, France.

0148-0227/03/2001JD001443$09.00

existing, low spectral resolution instruments [*Chédin et al.*, 2002a] with the NOAA TIROS-N Operational Vertical Sounder (TOVS). Using a set of radiosonde observations colocated with NOAA-10 observations, the measured TOVS radiances have been simulated with an accurate forward radiative calculation and a fixed specification of trace gases. An analysis of the differences between the measured and simulated TOVS brightness temperatures clearly reveals the signatures of multiyear trends and seasonal variations of CO_2, CO, N_2O, consistent with the line-by-line calculations of the effect of observed variations in the trace gases. Recently, these signatures have been interpreted in terms of CO_2 concentrations over a time period of about 4 years [*Chédin et al.*, 2002b] consistent with our present knowledge of the CO_2 atmospheric distribution. Various proposals have been made for measuring CO_2 from space both using reflected ultraviolet radiation [e.g., *Buchwitz et al.*, 2000] and Fourier transform spectrometry [e.g., *Park*, 1997].

[5] The Infrared Atmospheric Sounding Interferometer (IASI), with its numerous channels and its high spectral resolution, used synergistically with the Advanced Microwave Sounding Unit (AMSU), is one of the potential instrument combinations for monitoring of atmospheric CO_2 concentration from space. The Atmospheric InfraRed Sounder, AIRS, launched on the NASA Aqua polar orbiting platform is another instrument capable of monitoring CO_2 in the near future. This paper describes studies applied to simulated IASI data to investigate its capabilities to monitor atmospheric CO_2 concentrations from space [see also *Chédin et al.*, 1999] and studies of simulated AIRS data to derive the information content of a subset of AIRS channels [see also *Engelen et al.*, 2001]. These results are in general applicable to other high-resolution infrared sounders that have been launched or are planned in the next decade.

[6] In parallel with the provision of these new measurements from space, efforts are also underway to prepare atmospheric models to assimilate this information using 4D variational methods [e.g., *Klinker et al.*, 2000] currently successfully being employed for assimilating temperature, water vapor and ozone information into NWP model analyses.

[7] The paper is organised as follows. The natural variability of CO_2 is documented in section 2, the current measurements of CO_2 are described in section 3 and the sensitivity of IASI radiances to CO_2 is presented in section 4. The information content study of AIRS measurements is described in section 5. Finally in section 6 the role of ancillary data sources in improving the retrievals of CO_2 is described.

2. The Temporal and Spatial Variability of Atmospheric CO_2 Concentration

[8] The atmospheric CO_2 concentration is monitored by a network of ground stations of increasing density since the late 1950s. Since *Keeling* [1960] started the first monitoring station in 1958 at Mauna Loa (Hawaii), a network has evolved to more than 120 stations. They are far from being evenly distributed, the network being much denser in the Northern Hemisphere. The ground stations are complemented by programs of repeated measurements along ship tracks and onboard aircraft to get vertical profiles.

[9] These measurements are either made continuously (sampling rate $\sim$1 min) or by taking air samples in flasks, which are later analysed in the laboratory (sampling every one or two weeks). The CO_2 concentration measurements of the ground stations have been compared and the accuracy is estimated as 0.1 ppmv for monthly means, some stations being biased by a few tenths of ppmv. The ^{13}C measurements have not been compared, but this is now underway. The best accuracy achievable is 0.03‰ [*Keeling et al.*, 1989; *Francey et al.*, 1990; *Trolier et al.*, 1996]. The measurements, including paleo-measurements obtained from ice cores, are accessible in the database of the Carbon Dioxide Information Center (CDIAC). The existing data have been analysed and extended to provide a homogeneous database intended for modellers using atmospheric transport models to constrain sources and sinks of CO_2 at a global scale.

[10] The space and time characteristics of atmospheric CO_2 concentration can be described by the superposition of variations at different space and timescales. At global scales a trend due to anthropogenic inputs of CO_2 to the atmosphere is observed with the concentration increasing with time at 1.55 ± 1 ppmv year^{-1}; averaged between 1980 and 1992 [*Conway et al.*, 1994], the extreme values of the annual variation during this period being 0.60 and 2.46 ppmv. Spatially the variations are mainly meridional with a general north-south gradient of about 3.5 ppmv between the north pole (maximum) and the south pole (minimum), this gradient varying from year to year between 3 and 4 ppmv. Large-scale spatial variations of small amplitude, about 1 ppmv, are also observed over the ocean in regions of high air-sea exchange. At shorter timescales a seasonal variation mainly due to the photosynthetic activity of the terrestrial biosphere is observed. Its amplitude is a maximum around 65°N (about 16 ppmv) and decreases to the south. In the southern hemisphere the seasonal variation is of much smaller amplitude and is influenced by the air-sea exchange as well as by the terrestrial biosphere. Figure 1 shows the time evolution of the atmospheric carbon dioxide at different latitudes. A synthesis of these observations with a complete bibliography can be found by *Enting and Pierman* [1993] and in *Bousquet* [1997a] for more recent results.

[11] At timescales from a few hours to a few days a larger signal is observed. These synoptic variations are due to the meteorological activity that brings to the observing site continental airmasses. For instance when this air comes from industrialised countries they have CO_2 concentrations up to 20 ppmv above the usual concentration in the marine boundary layer as at Mace Head, Ireland [*Bousquet et al.*, 1997b]. Negative anomalies of the order of 5 ppmv coming from oceanic areas are also observed at this site due to variations of the airmass. Far from continents much weaker synoptic signals are observed. For instance at Amsterdam Island the amplitude of these events coming from South Africa is approximately $\pm$1 ppmv [*Gaudry et al.*, 1990]. Such plumes of different CO_2 concentrations simulated by atmospheric transport models are typically 10 degrees wide.

[12] As far as vertical gradients above the ocean are concerned, little is known since only a few aircraft sampling programs have been conducted. *Nakazawa et al.* [1991]

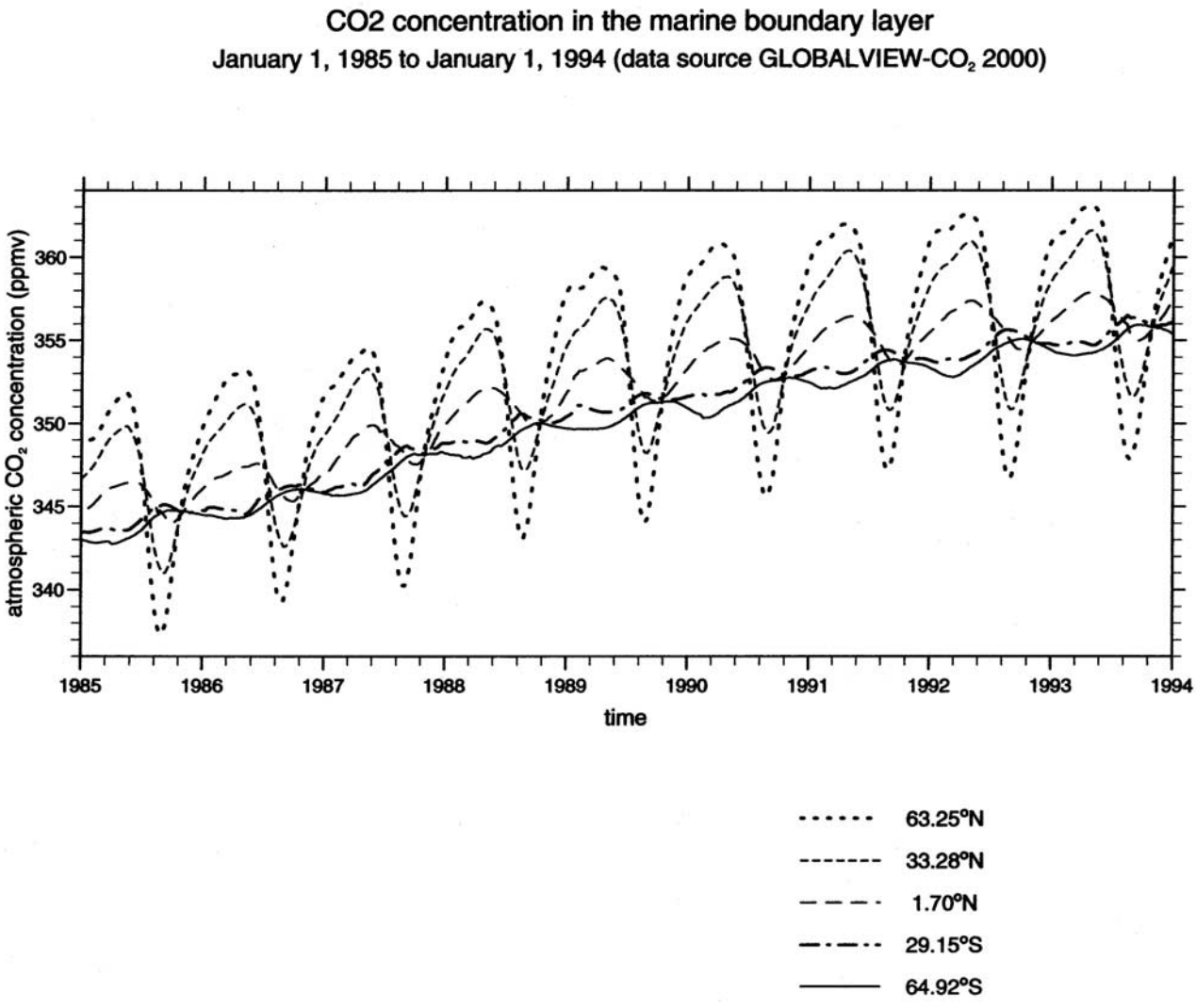

Figure 1. Evolution of atmospheric CO_2 concentrations from 1985 to 1994 at different latitudes [*GLOBALVIEW-CO_2*, 2000].

reported the results of an aircraft program between Japan and Australia. Some of their results are summarized in Figure 5 of *Enting and Pierman* [1993]. Recent results from flights above southeast Australia have established a climatology of these vertical profiles up to 8 km [*Pack et al.*, 1996; updated in *Pack et al.*, 1998]. Over the oceans the variations with altitude are of the order of 1 ppmv although larger differences are possible between boundary layer, free troposphere and stratosphere. Not enough measurements are available at present to be sure this is a globally applicable value.

[13] As far as the isotopic composition is concerned, about 1% of the atmospheric CO_2 is composed of $^{13}CO_2$. The isotopic composition is usually expressed in $\delta^{13}C$, where

$$\delta^{13}\mathrm{C\ meas.} = \left(\left(\left({}^{13}\mathrm{C}/{}^{12}\mathrm{C}\right)\mathrm{meas.}/\left({}^{13}\mathrm{C}/{}^{12}\mathrm{C}\right)\mathrm{ref}\right) - 1\right)*1000,$$

where $\delta^{13}C$ is expressed in ‰. The reference ratio is $(^{13}C/^{12}C)ref = 0.0112372$.

[14] The isotopic ratio gives indications of the influence of the terrestrial biosphere since photosynthesis and respiration provide an isotopic fractionation. Its seasonal cycle, mainly observed in the northern hemisphere, has an amplitude of about 1‰ and is out of phase with the CO_2 concentration seasonal cycle. The north-south gradient is about 0.2‰, $\delta^{13}C$ having a minimum at northern latitudes [*Trolier et al.*, 1996]. A general trend due to the fossil fuel input to the atmosphere is observed, $\delta^{13}C$ decreasing by 0.02‰ $year^{-1}$.

[15] These measurements of atmospheric CO_2 concentration and isotopic composition are used together with atmospheric transport models to identify and quantify sources and sinks of CO_2 to the atmosphere. Several models have been developed. *Tans et al.* [1990] and *Ciais et al.* [1995] have used a two dimensional (latitude/height) model. M. Heimann developed a three dimensional transport model that is widely used, at various spatial resolutions [*Heimann and Keeling*, 1989; *Heimann*, 1995]. Many others have also been developed. Inverse models are used to quantify CO_2 sources and sinks [*Bousquet et al.*, 1999; *Rayner et al.*,

Table 1. Summary of Advanced Sounder Instrument Characteristics

Parameter	Advanced Sounder			
	IMG	AIRS	IASI	CrIS
Instrument Type	Interferometer	Grating Spectrometer	Interferometer	Interferometer
Satellite Agency	NASDA	NASA/JPL	EUMETSAT/CNES	NOAA IPO
Spectral Range (cm^{-1})	600–3030	649–1135; 1217–1613; 2169–2674	Contiguous 645–2760	650–1095; 1210–1750; 2155–2550
Number of Channels	59623	2378	8461	~1300
Unapodised Spectral	10000–20000	1000–1400	2000–4000	900–1800
Resolving Power/ Spectral Sampling (cm^{-1})	0.03–0.04 cm^{-1}	~ν/2400	0.25 cm^{-1}	0.625/1.25/2.5 cm^{-1}
Spatial Footprint (km)	8	13.5	12	14
Nominal Altitude (km)	800	705	833	824
Sampling Density Per 50 km^2	1/86 km on track	9	4	9
Power (W)	150	225	200	86
Mass (kg)	115	176	230	81
Platform	ADEOS	Aqua	Metop-1/2/3	NPP and NPOESS
Nominal Launch Date	17 August 1996	4 May 2002	2005	2006(NPP), 2009(NPOESS)

1999]. The horizontal resolution of these models varies between 10° × 10° and 1° × 1° (see *Bousquet et al.*, 1997, for a more complete description).

[16] Satellite measurements could be used by such models to study sources and sinks at a global scale, as an interpolation between ground stations. The ground measurements could provide an absolute calibration removing any regional biases in the satellite data, which provide the space and time gradients provided the relation between the boundary layer CO_2 mixing ratios and the free troposphere is well known. In a preliminary test, *Rayner and O'Brien* [2001] using the method of synthesis inversion estimated that a satellite measuring monthly the column integrated CO_2 concentration over the ocean at 8° × 10° resolution would need a precision better than 2.5 ppmv (1.5 ppmv over the ocean) to constrain the inversion better than the surface network. *Peylin et al.* [2001] state a requirement of better than 1% of the mean mixing ratio (3–4 ppmv) for an area of 7.5° (longitude) × 7.2° (latitude). For the purposes of this paper we assume a measurement accuracy of 1% of the mean mixing ratio of CO_2 for a 500 × 500 km^2 area averaged over 15 days would be of use to the CO_2 monitoring community.

[17] Atmospheric transport models are also used to interpret synoptic variations. They are used to trace back the trajectories of the air masses arriving at the observing station [*Ramonet*, 1994; *Engardt et al.*, 1996] and determine their origin. Satellite measurements with an accuracy of 10 to 15 ppmv at a resolution of 7.5° and less than one day should allow these plumes to be observed directly. A simulation with a transport model would help to refine this estimate and give indications of the vertical structure.

3. High-Resolution Infrared Atmospheric Sounders

[18] Fourier transform spectrometers have been launched into space to record atmospheric spectra using either a limb-viewing geometry for stratospheric and upper tropospheric soundings, or a nadir-viewing mode for remote sensing of the troposphere. New instruments based on this technology will fly on polar-orbiting satellites within the next decade, for numerical weather prediction (NWP), climate and chemical composition studies. The analysis of each atmospheric spectrum provides information on the atmospheric state (temperature and composition) at the location of the measurement. Important regions of the spectrum measured are the vibrational-rotational CO_2 lines, which provide the atmospheric temperature information.

[19] Some of the current and planned high-resolution advanced infrared sounders are listed in Table 1. The Infrared Atmospheric Sounding Interferometer (IASI) is scheduled for launch in 2005 onboard the European METOP-1 platform. It is a high-resolution Fourier transform spectrometer designed to record atmospheric spectra using thermal emission from the atmosphere/surface. A precursor of this mission was the Interferometric Monitor for Greenhouse Gases (IMG) instrument [*Kobayashi et al.*, 1999a, 1999b], launched on the Japanese Advanced Earth Observing System (ADEOS) in August 1996. Ten months of data are available, until the satellite stopped operating (June 1997) due to the failure of its solar panels. The Atmospheric InfraRed Sounder, AIRS, was launched on the NASA Aqua polar orbiting platform [*Aumann and Pagano*, 1994] in May 2002. The notable difference between AIRS and IASI is that the radiometric noise is much less (~0.1K) for AIRS in the 4.4 micron CO_2 band because of its actively cooled detectors. The Cross-track Interferometric Sounder (CrIS) is scheduled to fly on the NPOESS (National Polar-orbiting Operational Environmental Satellite System) Preparatory Program (NPP) satellite in a similar timeframe to IASI and also on the operational NPOESS satellites themselves at the end of the decade. Unlike IASI it does not sample the entire spectrum but 3 parts as defined in Table 1 and the spectral sampling and resolution for CrIS is lower than for AIRS and IASI.

[20] The results presented in this paper refer to simulated IASI and AIRS data and measured IMG data. They have different spectral resolutions, and spatial and temporal sampling due to their different objectives, which are climate/chemistry research for IMG and operational NWP for IASI and AIRS. This results in a trade-off between spectral resolution and horizontal sampling. The IMG spectrometer records atmospheric spectra using an optical path difference (OPD) of 10 cm, which corresponds to an apodized spectral resolution of 0.1 cm^{-1}, whereas IASI uses an OPD ranging

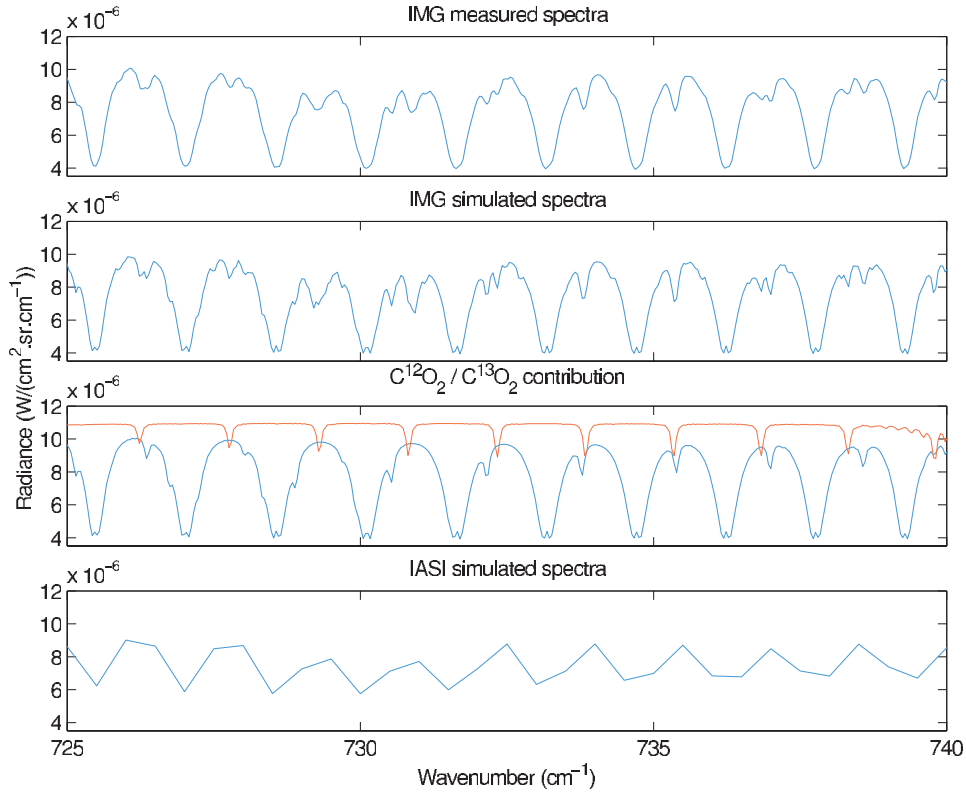

Figure 2. CO_2 absorption in the 725–740 cm^{-1} spectral range. The panels show the IMG measured spectra, the IMG and IASI simulated spectra, and separated contributions from $^{12}CO_2$ and $^{13}CO_2$, respectively, at the IMG spectral resolution.

from −2 cm to +2 cm, leading to a spectral resolution of about 0.5 cm^{-1} for apodized spectra. The difference in spectral resolution is illustrated in Figure 2, which shows calculated nadir radiances obtained at each instrumental resolution in the 15μm CO_2 absorption band, as well as a spectrum measured by IMG.

[21] IASI has a field of view, coincident with AMSU-A, sampled by a matrix of 2 × 2 circular pixels of 12 km each and will provide measurements with a good horizontal coverage due to its ability to scan across track with a swath width of 1100 km, whereas IMG only provides nadir measurements with a footprint of 8 × 8 km. For technological reasons, the full spectral range covered by these instruments is subdivided in three spectral bands with different radiometric noise associated with the performance of each detector. The latest estimate of the noise for IASI is plotted in Figure 3 from *Cayla* [2001].

[22] Atmospheric spectra recorded by the IMG have been analysed by different groups either for the retrieval of temperature and water vapor [*Amato et al.*, 1999; *Lubrano et al.*, 2000] or inversion of trace gas concentrations [*Clerbaux et al.*, 1999; *Hadji-Lazaro et al.*, 1999; *Turquety et al.*, 2002]. All these papers report the good quality of recorded spectra but highlight the lack of ancillary data required to perform accurate retrievals. A detailed instrumental spectral response function is not available, and cloud contamination information is not provided, but may be derived directly from the radiance spectra [*Hadji-Lazaro et al.*, 2001]. To the best of our knowledge, no studies have been reported on direct measurements of CO_2 using these spectra, which would require global scale accurately measured temperatures and surface emissivities. Furthermore, as discussed in section 2, the maximum CO_2 seasonal variability (∼16 ppmv at midlatitudes) is expected between mid-April and end of August. But as the ADEOS platform stopped operating at the end of June, the IMG data is not ideal to observe this maximum amplitude of the variation.

[23] Another interesting possibility is to study the ratio of $C^{13}O_2$ versus $C^{12}O_2$, which, as explained in section 2, provides an indication of the CO_2 sources and sinks. The high spectral resolution provided by the IMG instrument allows the spectral contribution of $C^{12}O_2$ in the rotational vibrational ν_2 band to be distinguished from other absorbing contributions in hot bands and isotopes. Figure 2 shows the absorption contribution from the different isotopes in the 725–740 cm^{-1} spectral range, which was found to be the optimal spectral range to study isotopic composition. Although the absorption features are clearly seen, small variations of the isotopic ratio may be difficult to retrieve. These retrievals are not possible with apodised IASI spectra as can be seen in Figure 2.

4. Sensitivity Studies for IASI Measurements

4.1. Radiative Transfer Models Used for Simulations

[24] To investigate the potential for IASI to detect CO_2 changes from top of atmosphere radiance measurements two independent sets of simulations, using different models, were performed to determine how much the radiances are changed by varying the CO_2 concentration by typical

amounts. In addition atmospheric temperature, water vapor, ozone and nitrous oxide profiles and surface emissivity and temperature were also varied to gauge their effects on the radiances. The results from both simulations were similar giving confidence in them. Both radiative transfer models are described briefly below.

[25] First the line-by-line atmospheric transmittance and radiance code, GENLN2 [*Edwards*, 1992], was used with line parameters from the 1996 version of the High-Resolution Transmission (HITRAN) molecular database [*Rothman et al.*, 1998]. Carbon dioxide line coupling was modelled using the line coupling coefficients included [*Strow et al.*, 1994]. Spectra were computed at 0.001 cm^{-1} resolution and then convolved with the appropriate [*Cayla*, 1996] IASI Spectral Response Function (ISRF) to obtain the level 1C IASI apodized spectra. The transmittance calculations were made on 43 fixed pressure levels from 0.1 to 1013 hPa. For the radiance stage of the line-by-line computations, the surface temperature was set equal to the 1013 hPa value of the temperature profile and a value of 0.98 was assumed for the surface emissivity. This value is expected to cover a broad range of surface classes for the frequencies of interest in this study [*Snyder et al.*, 1988]. Radiances were simulated for subarctic winter, midlatitude summer, midlatitude winter and tropical profiles taken from the AFGL set of atmospheric constituent profiles.

[26] To complement the above, similar computations were carried out using the Automatized Atmospheric Absorption Atlas (4A) fast line-by-line transmittance and radiance computation model [*Scott and Chedin*, 1981] in its latest 2000 version. 4A relies on the use of a vast archive (the atlas) of optical depths created, once and for all, using the line-by-line and layer-by-layer model, STRANSAC, [*Scott*, 1974; *Tournier et al.*, 1995] in its latest 2000 version with up-to-date spectroscopy from the GEISA spectral line catalogue [*Jacquinet-Husson et al.*, 1999]. Spectra were computed at a resolution of the order of the smallest line half-width (about 5.10^{-4} cm^{-1}) and then convolved with the IASI response function (unapodized). Transmittance computations were made on 40 pressure levels from 1013 hPa to 0.05 hPa. The surface emissivity varied with frequency according to *Masuda et al.* [1988] for seawater. The results using GENLN2 are shown in Figures 3–7 and 4A in Figure 8.

4.2. Sensitivity to Changes in CO_2 Concentrations

[27] The reference spectra were computed assuming a climatological concentration value for CO_2 equal to 376 ppmv. This is the predicted concentration value for the year 2005 assuming an annual mean CO_2 mixing ratio of 356 ppmv for the year 1992 [*Conway et al.*, 1994] and a yearly increase rate of 1.5 ppmv [*Schimel et al.*, 1995]. For each profile considered in the study, test spectra were computed by perturbing the annual mean CO_2 mixing ratio profile by half the value of the mean peak-to-peak amplitude of the seasonal CO_2 cycle (for GENLN2 only the tropospheric amount was perturbed). This is 9 ppmv for midlatitude and subarctic winter profiles and 4 ppmv for the tropical profile [*Conway et al.*, 1994]. As a result of this, the CO_2 mixing ratios used in the computations were 380 ppmv for the tropical profile, 385 ppmv for the midlatitude winter and subarctic profiles, and 367 ppmv for the midlatitude summer profile. Figure 3 shows, for the above profiles, the difference in radiance between the reference and perturbed CO_2 case for the frequency range 650 to 850 cm^{-1} (hereafter referred to as LW) in the upper panel. The radiance difference for all the plots is expressed in terms of the equivalent brightness temperature difference, at a reference blackbody temperature, which is the mean scene temperature at each wavelength (i.e., average of all simulated spectra). This can be directly compared with the instrument noise also plotted, which is the estimated IASI radiometric noise at the reference temperature [*Cayla*, 2001].

[28] For the midlatitude winter and midlatitude summer profiles the predicted change in radiance is 0.25K just above the noise. Smaller values are observed for the subarctic winter ($\sim$0.2 K) and tropical profile ($\sim$0.1 K). Note that the noise curve plotted in Figure 3 is the noise for a single IASI pixel. As the signal is only at the level of detectability an averaging of the IASI retrievals will be necessary for a CO_2 retrieval to be possible. Another option would be to retrieve CO_2 as part of the routine assimilation process of a NWP model, and then average the daily retrieved CO_2 fields. Results are also shown for the spectral region 2200 to 2500 cm^{-1} (hereafter referred to as SW) in Figure 3. In this case the signal (predicted changes in brightness temperature) peaks at +0.3K (for midlatitude winter profiles) and up to -0.3K (for the midlatitude summer profile). This is well below the instrument noise at 2250 cm^{-1} for a single IASI pixel measurement.

[29] In addition to perturbing the entire profile, which is not a change encountered in nature, runs were also made where only the 700–200 hPa layer was perturbed and also the 700 hPa-surface was perturbed. The results (not shown) clearly show nearly all the radiance signal comes from changes in CO_2 concentration in the 700–200 hPa layer not the layer close to the surface so that IR sounders will not be suitable for monitoring changes of CO_2 in the atmospheric boundary layer. This is also illustrated by the AIRS CO_2 jacobians referred to later.

4.3. Sensitivity to Changes in Temperature, Humidity, and Other Minor Gases

[30] The influence of uncertainties in temperature and humidity on the CO_2 retrieval was quantified by perturbing the mean temperature and humidity profiles by an amount given by the mean error in the background (from a 6 hour forecast) ECMWF model fields for each latitude band. This represents the ''background'' error assumed in the retrieval/assimilation schemes. These errors in temperature and specific humidity were taken from the 1999 version of the ECMWF 50 level model analysis system. It is likely that future developments in data assimilation, NWP model formulation and increased use of satellite data will reduce these errors so those assumed here are an upper limit. For each of the atmospheres considered in the study a different mean error profile was used. The error varies with level, the typical range being 0.8K at the surface to 3K in the stratosphere for temperature and 2000 to 0.02 ppmv for water vapor mixing ratio. The profiles used in the perturbed cases were obtained by increasing the reference profiles by the mean error profile for that atmosphere. Note this implies full vertical correlation of the errors, which is not a realistic

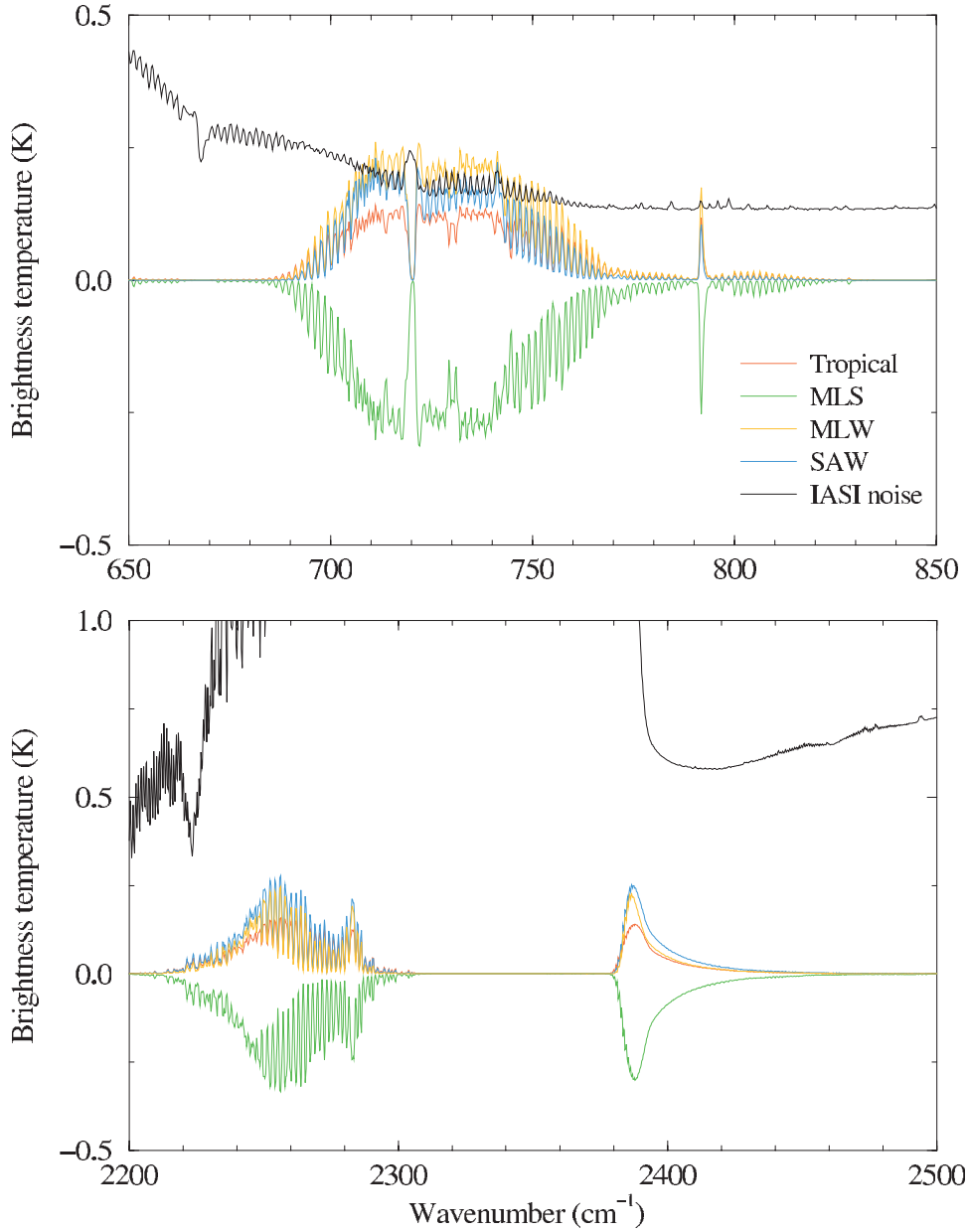

Figure 3. Response of simulated IASI radiance spectrum to changes in CO_2 concentration for 4 different standard atmospheres. The upper panel shows the response in the LW band, and the lower panel the response in the SW band.

assumption but gives an upper limit to the effect of uncertainties in the atmospheric profile.

[31] For temperature the results are shown in Figure 4 where for each of the atmospheres the radiance difference between reference and perturbed case is shown. For all atmospheres, perturbing the temperature profile gives a signal greater than that obtained by perturbing the CO_2 profile. For the LW region of the spectrum (upper panel of Figure 4) the uncertainty due to temperature gives a signal three times greater than the CO_2 signal. The SW region (lower panel of Figure 4) is less sensitive to temperature uncertainties, due to the nonlinearity of the Planck function, but still gives a signal about twice that of the CO_2 changes.

[32] The effect of CO_2 anomalies is likely to be a bias, whereas the signal from the perturbed temperature profile in general is expected to be randomly distributed, over a reasonable time period (~2 weeks) and should average out when a large sample of IASI radiances is considered. However, there are conditions in some locations where the temperature errors in the model and CO_2 errors may be correlated and this will need to be studied in more detail with in-situ data.

[33] The sensitivity of the radiances to the perturbation of the humidity profile is shown in Figure 5. As for the temperature sensitivity, the signal resulting from the perturbation of the humidity profile can be several times greater than the signal from the CO_2 variation. However, it is worth noting that several regions free from water vapor interference can be identified (e.g., 721 cm^{-1} for the LW and beyond 2245 cm^{-1} for the SW) where the effect of water

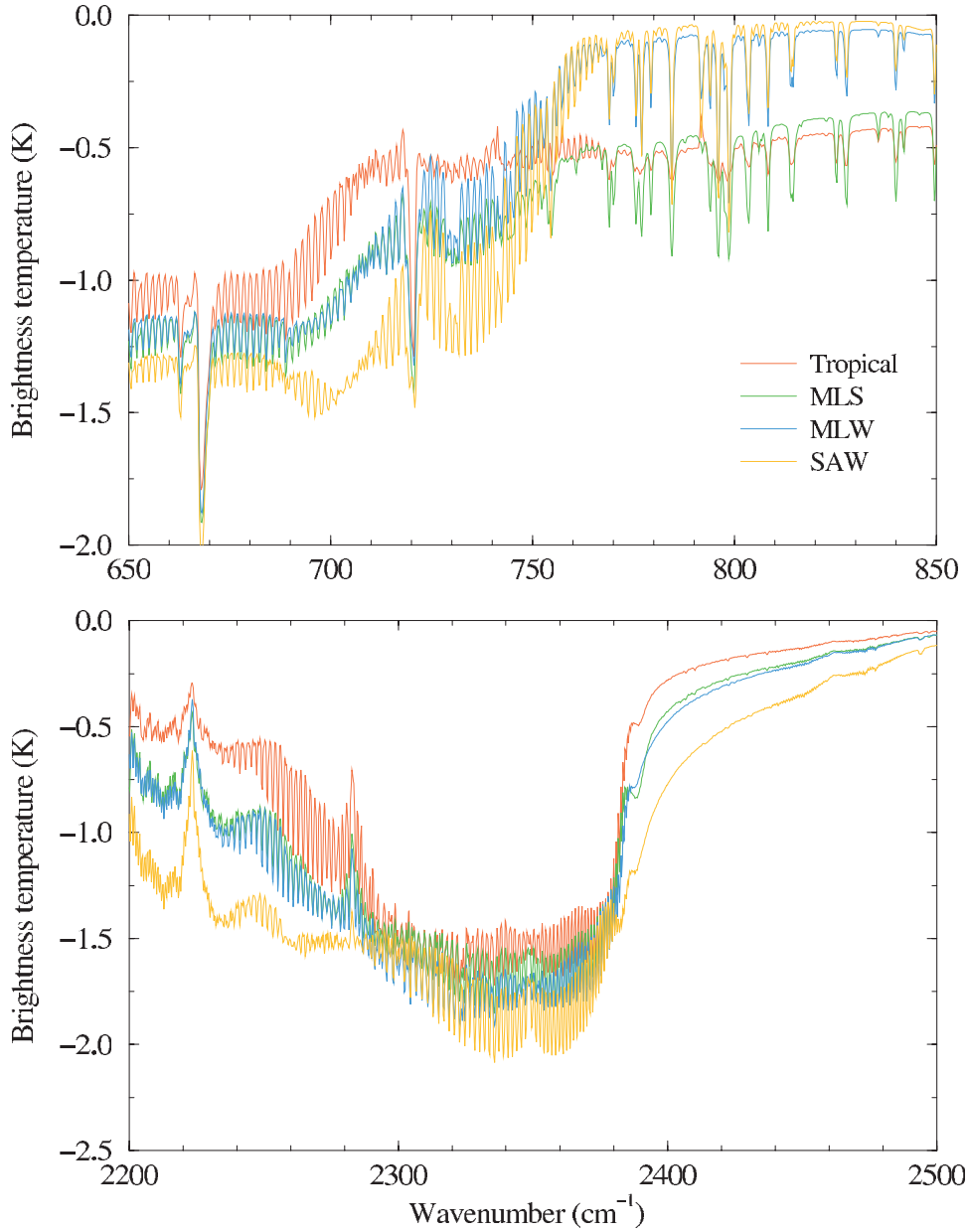

Figure 4. Response of IASI radiance spectrum to changes in temperature, equivalent to ECMWF background errors, for 4 different standard atmospheres. Note the surface temperature is modified by the same amount as the lowest atmospheric level.

vapor is negligible or absent in this part of the spectrum. This suggests the parts of the spectrum that are not sensitive to water vapor should be used for the CO_2 retrieval. Unfortunately the 720 cm^{-1} region is in a strong CO_2 absorption band insensitive to tropospheric CO_2.

[34] For the sensitivity to uncertainty in ozone concentrations Figure 6 shows the radiance response for a midlatitude summer atmosphere (474 Dobson units) when the ozone amount is reduced by 13.5%, which is a typical magnitude of the variability in ozone at midlatitudes. In the LW region the peak radiance perturbation is −0.7K close to 725 cm^{-1} but there is a window at 720 cm^{-1}. In the SW the sensitivity to ozone becomes negligible above 2240 cm^{-1}.

[35] The sensitivity to nitrous oxide, N_2O, was checked by comparing the mean of the US standard atmospheres N_2O concentration with the tropical profile. The results are shown in the lower panel of Figure 6. There are no significant absorption bands due to N_2O below 1100 cm^{-1} so the LW region is unaffected. In the SW region there is a sensitivity, which reduces to zero at 2255 cm^{-1}. No sensitivity to methane was found in these spectral regions. Carbon monoxide does absorb from 2150–2200 cm^{-1} in the same region as N_2O.

[36] In summary for the LW part of the spectrum temperature, water vapor and ozone all affect the same region of the spectrum as CO_2 making the choice of channels in this LW region not affected by either water vapor or ozone more difficult. In the SW only temperature affects the same region of the spectrum as CO_2 and to a lesser extent than in the LW. Hence although the sensitivity to CO_2 is less relative to

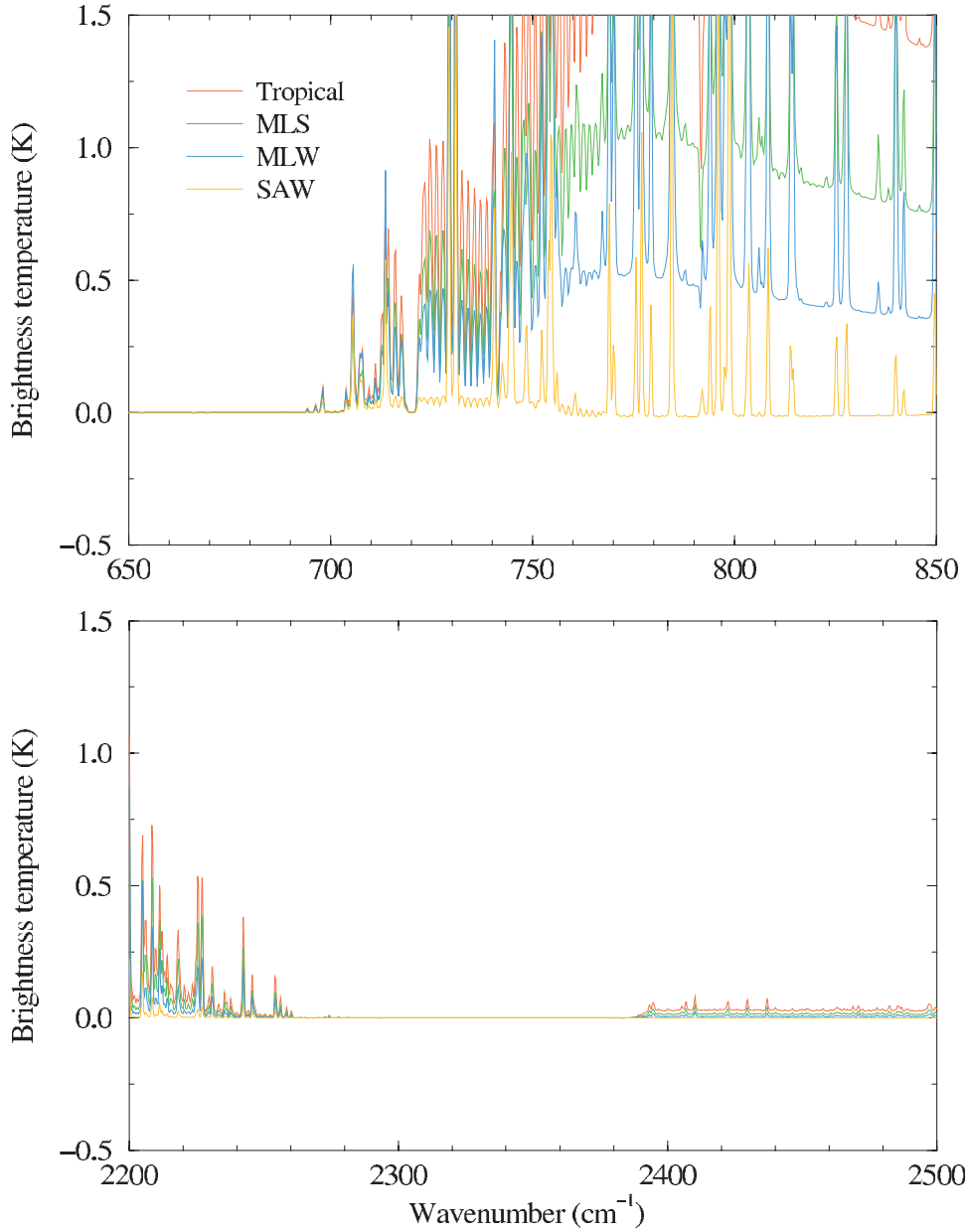

Figure 5. Response of IASI radiance spectrum to changes in water vapor concentration, equivalent to ECMWF background errors, for 4 different standard atmospheres.

the IASI noise in the SW there is less interference from other absorbing molecules there.

4.4. Sensitivity to Changes in Surface Temperature and Land Surface Emissivity

[37] This test was carried out only for the subarctic atmosphere as with low water vapor amounts this will give an upper bound to the sensitivity of the surface emissivity. The perturbed surface temperature was set equal to the reference value plus 1 K whereas the perturbed land surface emissivity was set equal to 0.97 a change of 0.01. Results are shown in Figure 7. For the 645 to 710 cm^{-1} wave number region the radiance is not sensitive to changes in emissivity whereas in the 710 to 745 cm^{-1} region the signal is still less than the CO_2 signal. The signal can be as great as +0.6 K. For the surface temperature case the radiance change is greater than the CO_2 signal for wave numbers greater than 720 cm^{-1}. In contrast, for smaller wave numbers the signal coming from the surface temperature perturbation is either zero or slightly less than the CO_2 signal. Elsewhere the signal peaks at −1K for the window regions. For the SW region the sensitivity to surface parameters becomes negligible at frequencies between 2250 and 2380 cm^{-1}. Over water the uncertainty in emissivity and temperature is much less making CO_2 retrievals over the ocean easier.

4.5. Impact of Errors in Spectroscopic Databases

[38] Persistent discrepancies are still observed between line-by-line-simulated and observed high-resolution spectra in some CO_2 and H_2O absorption bands. These errors are mostly due to the inaccuracies in the line intensities pres-

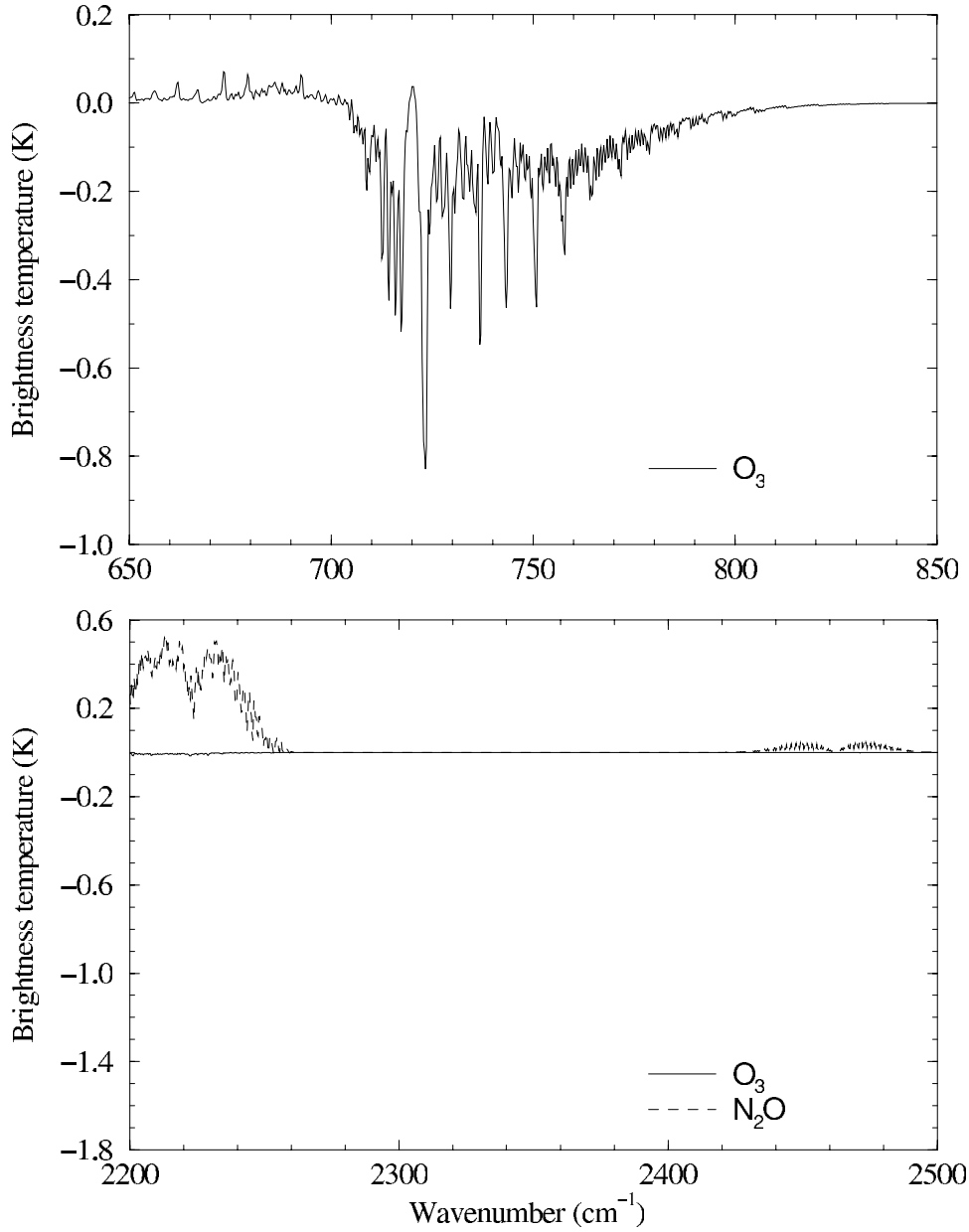

Figure 6. Response of IASI radiance spectrum to changes in ozone and nitrous oxide concentration, (see text for perturbations).

ently used and for CO_2 in the line mixing formulation. Difficulties also exist for measuring accurate in-situ atmospheric water vapor amounts to validate the spectroscopic parameters. These problems do not affect the conclusions on the relative amplitude of the signal due to CO_2 perturbations reported here. However, such limitations should be taken into account when selecting the best set of channels for monitoring CO_2.

4.6. Signal to Noise and Averaging

[39] The above results have illustrated the sensitivity of IASI to CO_2 perturbations. This section deals with the averaging required to obtain CO_2 profiles that differ significantly from the mean background field. Figure 8 shows the ratio of the IASI response to CO_2 perturbations to the IASI nominal noise, computed at the temperature "seen" by each channel (function of frequency), for the 4 atmospheric situations considered (tropical: perturbation of 4 ppmv; midlatitude winter and summer and subarctic winter: perturbation of 9 ppmv). A signal to noise of unity is reached for channels between 704 cm^{-1} and 745 cm^{-1} but for channels at 2250 cm^{-1} only values of 0.4 are reached for the midlatitude summer profile perturbation and a single measurement. Significant averaging is therefore required to raise the CO_2 signal-to-noise ratio.

[40] Over a 500 × 500 km^2 area there will be ~12,000 IASI measurements over a 15 day period of which ~25% would be expected to be insignificantly contaminated by cloud or aerosol giving 3000 useful measurements. This translates to a signal-to-noise ratio of >30 for the LW channels and >5 for the SW channels for a 1% change

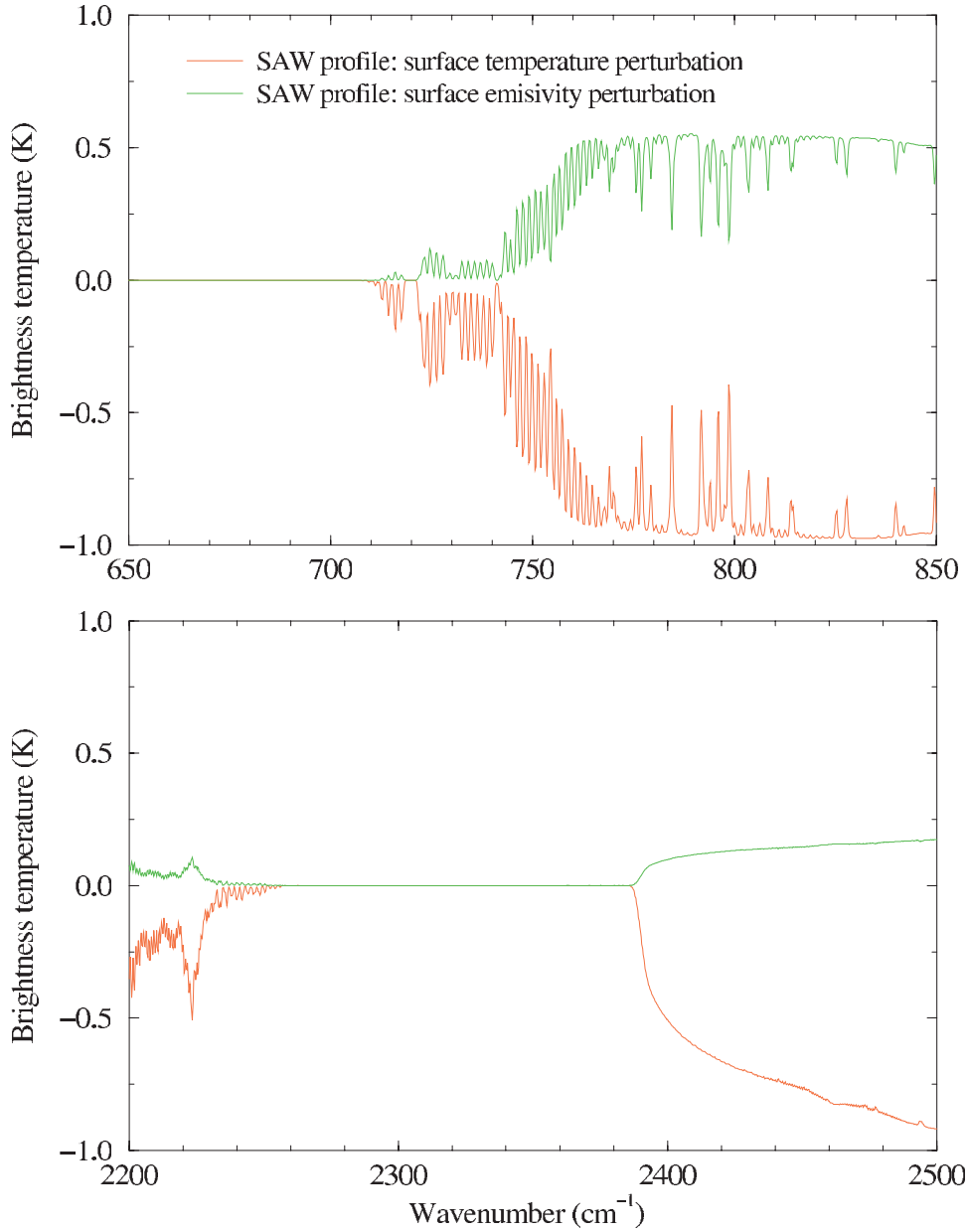

Figure 7. Response of IASI radiance spectrum to changes in only surface temperature or emissivity for the subarctic winter profile.

(3.8 ppmv) in total column CO_2 over 15 days. This is broadly consistent with the requirements for monitoring the atmospheric CO_2 concentration from space (see section 2). This will be a pessimistic estimate so long as the channels are uncorrelated the 'spectral averaging' through the use of many channels will improve the signal to noise further. This is taken into account in the information content study presented in section 5.

[41] To be successful, consideration must be given to selecting channels to minimize the "interference" from other atmospheric and surface variables. Channels not sensitive to surface characteristics are quite easy to select but channels not sensitive to water vapor and other minor gases are more difficult, but feasible, to identify. Signals coming from the temperature errors cannot be avoided but, as pointed out in section 4.3, the signal from CO_2 is likely to be a bias whereas the signal from errors in temperature is expected to be randomly distributed over a reasonable time period (~15 days). These constraints are compatible with studies at a global scale of the atmospheric CO_2 sources and sinks provided a 15-day mean accuracy approaching 1% of the total column amount can be obtained, which is a challenging but not impossible target for IASI measurements.

5. Information Content of AIRS Channels for CO_2 Retrievals

[42] For retrieving CO_2 from advanced IR sounders a subset of channels can be selected to reduce computa-

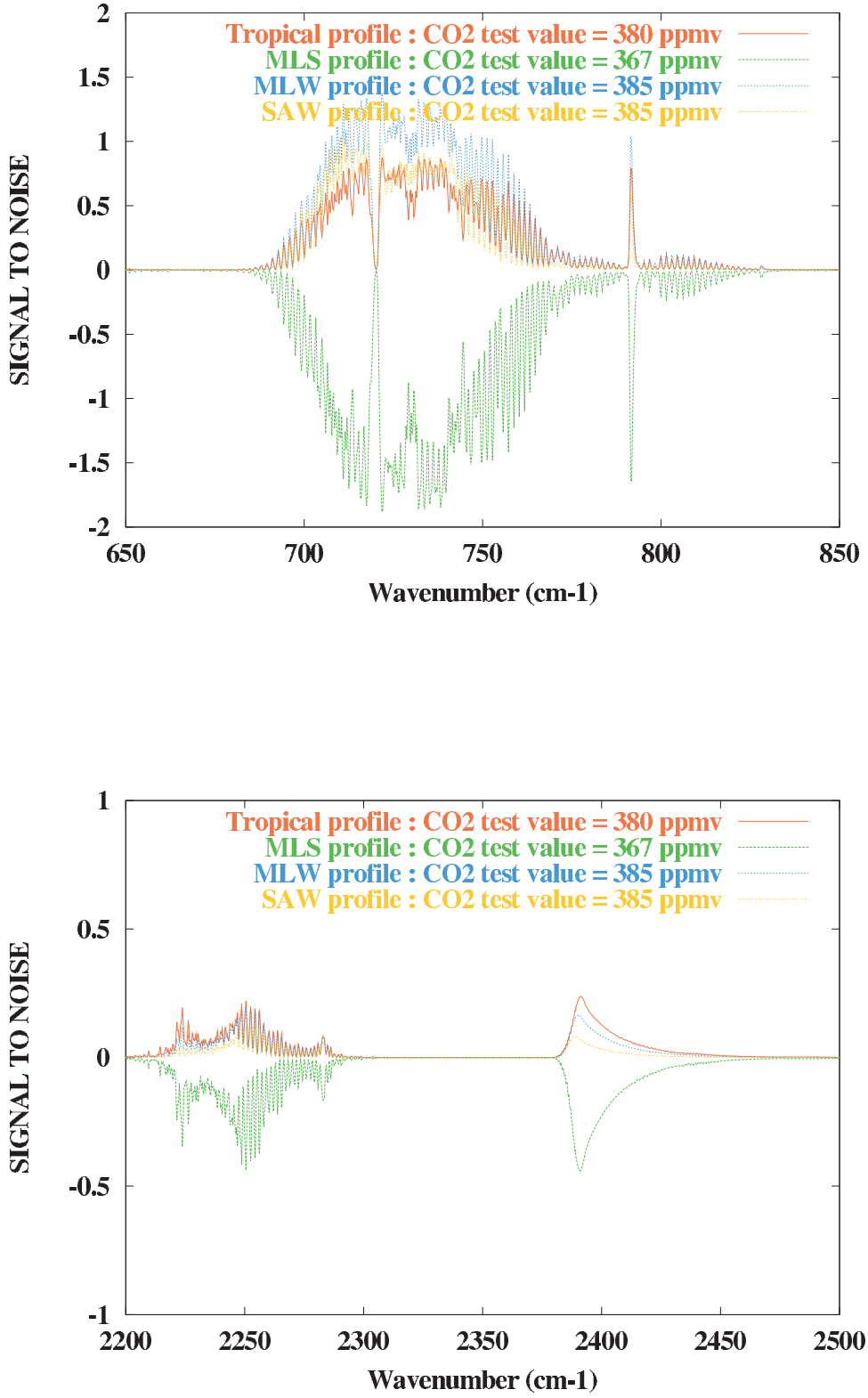

Figure 8. Signal (response of IASI to CO_2 changes) to noise (nominal IASI) ratio as a function of the wave number (cm^{-1}). Green: midlatitude summer; blue: midlatitude winter; red: tropical; orange: subarctic winter.

tional cost, which are optimal in the sense of retrieving CO_2. This section presents results of an information content study for different selections of AIRS channels. The method for channel selection uses linear optimal estimation theory as described by *Rodgers* [1996] and recently applied to IASI data for temperature and water vapor retrievals by *Prunet et al.* [1998] and *Rabier et al.* [2002]. If $\mathbf{x}^t$ is a vector that represents the true atmos-

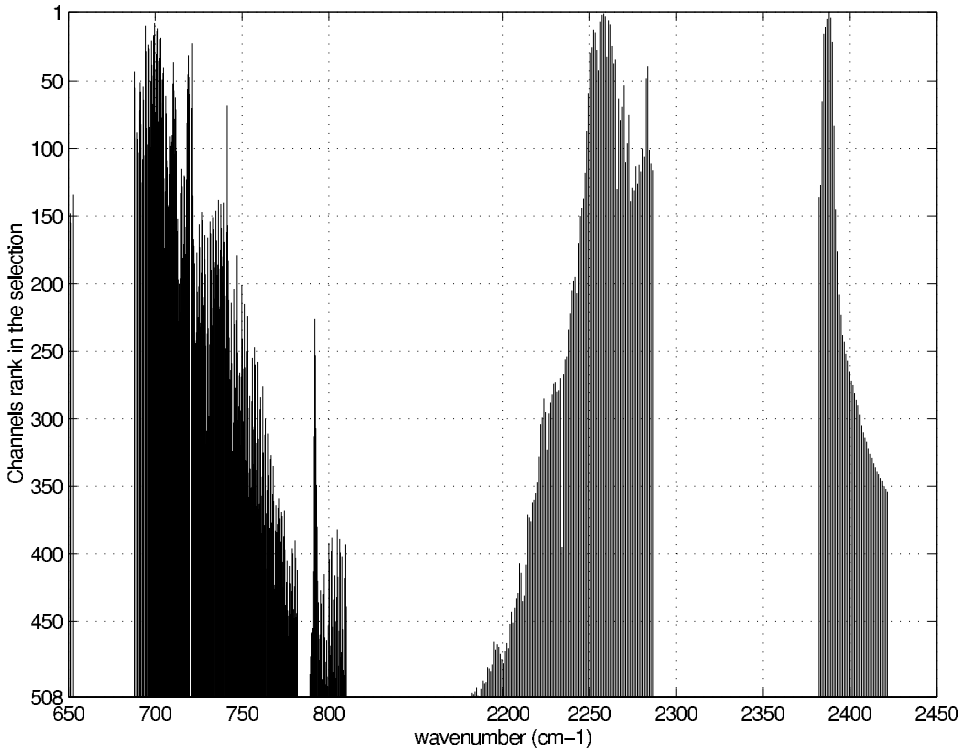

Figure 9. Spectral location of the selected AIRS channels for the AFGL tropical profile situation. The higher the value the more important the channel.

pheric state, then this is linked to the observations through the expression:

$$\mathbf{y}^0 = H(\mathbf{x}^t) + \varepsilon \tag{1}$$

where $\mathbf{y^o}$ is the observation vector (in this case AIRS channel radiances), ε is the observation + forward model error with a covariance $\mathbf{R}$ and H is the observation operator, which, in this case, is a radiative transfer model. The retrieved atmospheric state, $\mathbf{x^a}$, is the most probable estimate of $\mathbf{x^t}$ given the observations $\mathbf{y^o}$ and a background atmospheric state, $\mathbf{x^b}$, together with their respective error covariances $\mathbf{R}$ and $\mathbf{B}$. The retrieval error covariance matrix $\mathbf{A}$ is given by

$$\mathbf{A}^{-1} = \mathbf{B}^{-1} + \mathbf{H^T R}^{-1}\mathbf{H} \tag{2}$$

where $\mathbf{H}$ is the Jacobian of the radiative transfer model H. For channel selection the retrieval error covariances are iterated as each channel is selected:

$$\mathbf{A_i}^{-1} = \mathbf{A_{i-1}}^{-1} + \mathbf{H^T R}^{-1}\mathbf{H} \tag{3}$$

The gain in information content, S_j, with j varying over all the channels not selected is

$$S_j = \frac{1}{2}\ln|\mathbf{A_{i-1}}| - \frac{1}{2}\ln|\mathbf{A_i}| \tag{4}$$

assuming Gaussian statistics. For the first iteration ($i = 1$) the channel that brings the most gain in information from the background state $\mathbf{x^b}$ in terms of entropy reduction is chosen. A new state $\mathbf{x^i}$ with a new error covariance matrix $\mathbf{A_i}$ is obtained from the background and modified by the channel chosen. The next step is to choose another channel, which provides the most information from this new state, and then to iterate the method until the desired number of channels is reached.

[43] Results have been obtained for the AFGL profiles. The state vector $\mathbf{x}$ in this case is the tropospheric CO_2 profile. Temperature, water vapor, trace gases profiles and surface characteristics are assumed to be accurately known with any remaining uncertainties taken into account in the observation + forward model error. We assume the observation and forward model error covariance matrix, $\mathbf{R}$, is diagonal. For each channel, the instrument noise is computed for the atmospheric situation studied. The forward model used was the latest version of the 4A model described by *Garand et al.* [2001] and the error variance is assumed constant and equal to $(0.2)^2$ K^2 for all the channels, as assumed in *Prunet et al.* [1998] and other similar studies. The noise due to the residual uncertainties of water vapor, trace gases and surface characteristics are defined as the root mean square of the perturbations in brightness temperature shown in section 4. Our apriori knowledge of CO_2 profile concentrations is poor due to lack of measurements but it is a reasonable assumption that CO_2 concentration is almost constant in the troposphere. For simplicity we assume that the background error covariance matrix, $\mathbf{B}$, is diagonal with a constant variance taken equal to 10^2 $ppmv^2$ as we are not concerned here with stratospheric-tropospheric correlations, which may be important.

[44] We restrict our study to the channels of the CO_2 bands for which the tropospheric part of the CO_2 signal dominates. For the AFGL tropical profile, this results in studying the information content of 508 AIRS channels. Figure 9 shows the spectral location of the 508 channels for

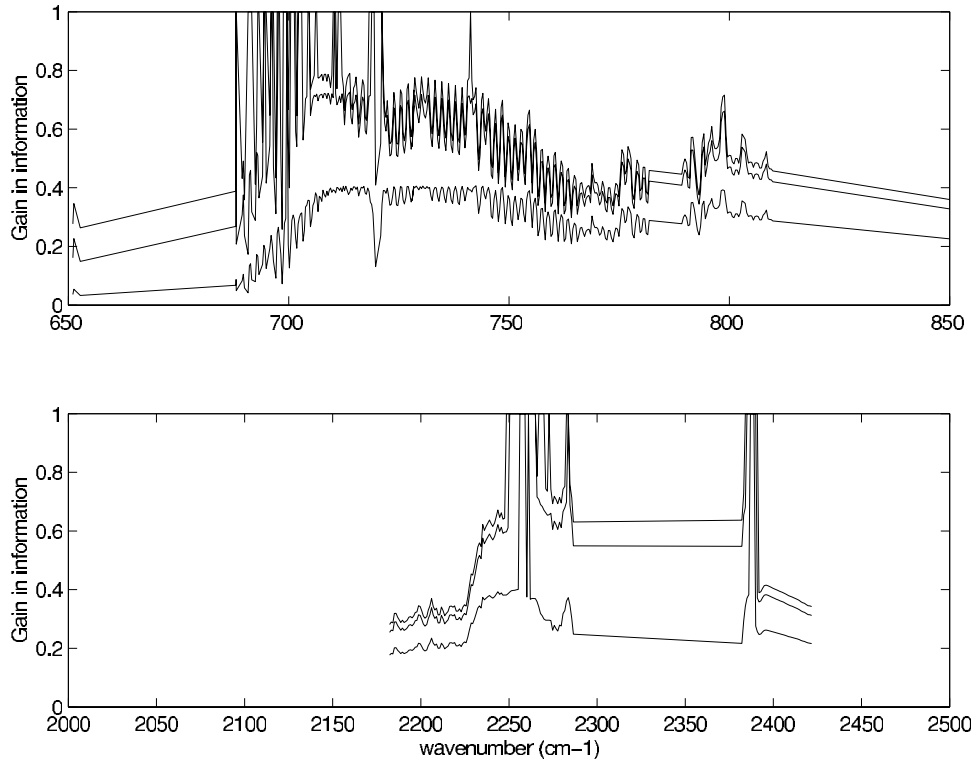

Figure 10. Gain in information from the 10 first (lower line), 50 first (middle line), and 90 first (upper line) selected AIRS channels for the AFGL tropical profile.

the tropical situation. Among them, the channel labeled 1 in the ordinate is the first to be selected: it is the one that brings the largest gain in information from the background. Selecting, for example, 10 channels retains the 10 highest vertical bars. The 508 channels form three spectral groups, which correspond to the spectral regions sensitive to tropospheric CO_2 as shown in Figure 3.

[45] To show the gain in information from the background state due to the selection of various channel selections the lines in Figure 10 correspond to the information gain obtained after the selection of the first 10, 50 and 90 channels that bring the most information about tropospheric CO_2. Note the gain in information with only 10 channels is significant but the increase in information in going from 50 to 90 channels is smaller.

[46] To determine which part of the atmosphere is observed by the first 10 selected channels, Figure 11 plots their CO_2 Jacobians for the AFGL tropical profile. A large part of the troposphere extending from about 100 hPa to 700 hPa is observed in deep layers, whereas the lower troposphere (700–1000 hPa) is not observed, which confirms the results in section 4.2. The Jacobians "covering" the lower part of the troposphere correspond to the first selected channels in the SW band.

[47] Information content studies have also been made comparing TOVS (19 HIRS channels) with AIRS (508 channels) for CO_2 retrievals. Between 100 and 300 hPa the gain in information content with AIRS over TOVS is greater than 10. Below 300 hPa this gain increases to ~100 at 700 hPa. Even if only the first 10 AIRS channels are used the gain over TOVS is significant especially at low levels.

[48] For tropical profiles, the first selected AIRS channels are in the SW part of the spectrum. Then channels are selected equally in each band. A similar study for the subarctic winter however predicts that more channels in the LW region are selected first for these profiles. This analysis was also run on the midlatitude AFGL profiles and when results for all profiles were considered they suggested around 50 AIRS channels in the SW and LW region were sufficient to extract most of the tropospheric CO_2 information for all atmospheric states. It should be noted that both SW and LW CO_2 bands are important for retrieving CO_2 in all situations. Finally, the new advanced instruments will allow us to cover the troposphere, from the tropopause to 700 hPa, with an improved gain in information compared to TOVS.

6. Evaluation of the Role of Ancillary Data

6.1. Independent Imagers for Cloud Detection and SST Retrieval

[49] One of the principal disadvantages of infrared sounders is that they are strongly affected by any cloud in the field of view. In order to ensure the radiances used for inferring CO_2 amounts are not contaminated by cloud, and hence give an erroneous retrieval, a higher resolution imager is useful to ensure all significant clouds can be detected. The Advanced Very High Resolution Radiometer (AVHRR), which has 1-km fields of view, will be on the same platform as IASI and can be used for cloud detection. It has visible channels and so during the day reflected sunlight can be used to discriminate between low clouds and sea surface. Another advantage of these imaging radio-

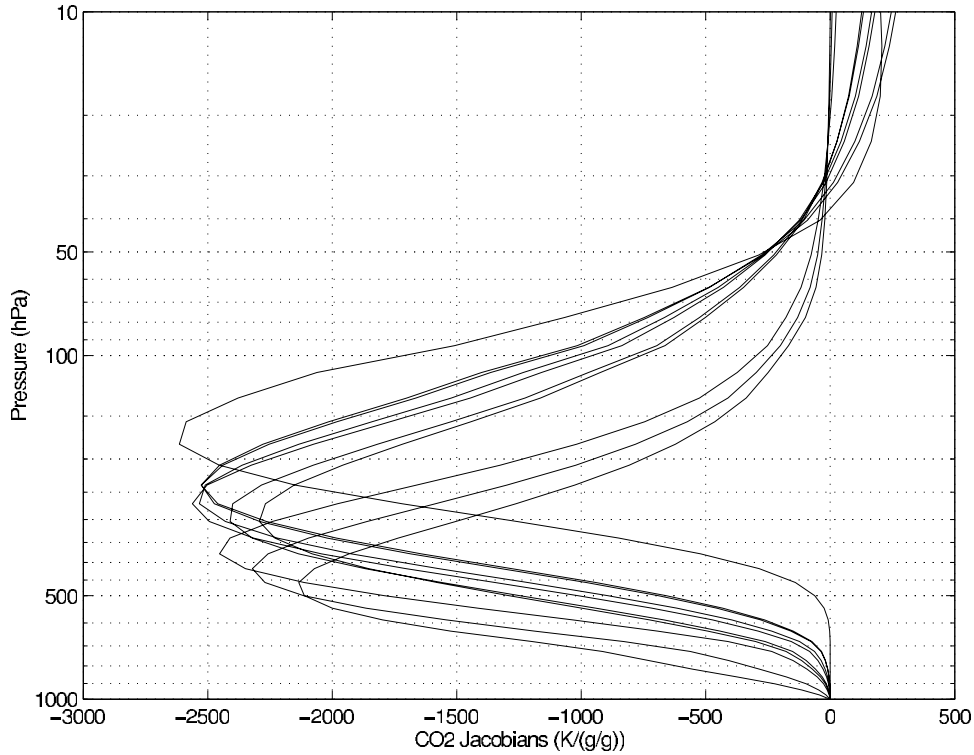

Figure 11. CO_2 Jacobians of the 10 first selected channels for the AFGL tropical profile.

meters is the radiometric noise is less than for IASI (e.g., 0.1 K for AVHRR versus 0.25K for IASI) allowing a less noisy radiance field for cloud detection. Similarly the Moderate Resolution Imaging Spectroradiometer (MODIS) can be used with AIRS.

[50] In addition, for the window channels, which are sensitive to the surface, it is important to have an accurate estimate of the sea or land surface temperature in order to have confidence in the retrieved CO_2 amounts. Accurate measurements of sea surface skin temperature (SSST) can be made using the IASI/AIRS window channels in a range of different wavelengths in cloudfree areas. However, there are problems with using the window channels to infer SSST as the 10 km field of view means cloudfree scenes over some parts of the ocean are rare. Imaging radiometers such as AVHRR and MODIS are more likely to "see" between the gaps in the clouds. This improved capability for cloud detection and coverage of cloudfree areas should improve the accuracy of the SSSTs and the CO_2 retrievals.

6.2. Synergy of AMSU and IASI/AIRS

[51] In order to be confident any change in CO_2 concentrations from advanced IR sounders are not just a consistent change in atmospheric temperature over the region of interest an independent measurement of atmospheric temperature must be made at the same time as the CO_2 retrieval. This is possible with the AMSU-A radiometer on METOP and Aqua, which sounds the atmospheric temperature using the 50–55 GHz oxygen absorption band in contrast to the CO_2 bands traditionally, employed in the infrared. Any changes in CO_2 concentration will not affect temperature profiles retrieved using the microwave oxygen absorption band.

[52] To determine exactly how sensitive the AMSU-A channels are to the temperature profile a radiative transfer model for the AMSU channels (RTTOV-5 as described by *Saunders et al.*, 1999) was used to compute top of atmosphere AMSU-A brightness temperatures for the same standard atmospheres used in section 4. The computation was carried out for the standard profile and then the whole profile was incremented by a constant value at all levels and a revised brightness temperature computed. The temperature increments applied to the profiles corresponded roughly to the change in temperature for each profile that was equivalent to the change in radiance seen in the infrared spectra for a seasonal change in CO_2. For example as Figure 12 shows for a midlatitude winter atmosphere the change in radiance due to CO_2 is about 0.2K and so this was the value by which the midlatitude winter profile was incremented for the AMSU-A calculations. The results for three latitude bands are shown in Figure 12 for AMSU channels 1–12 (the remainder do not sound the tropospheric temperature profile). A realistic sea surface emissivity for tropical and midlatitude winter profiles was assumed, and a constant value of 0.9 (for snow) for the arctic profile was used, which explains the different responses in the AMSU-A window channels (1–3). The response for the midlatitude and arctic profiles is twice that of the tropical profile (because of the larger seasonal variation in CO_2 at high latitudes) but in all cases is less than the specified instrument radiometric noise for each channel for a single radiance measurement. It is worth noting that the actual noise values for AMSU-A on NOAA-15 measured in the laboratory before launch were in many cases less than the specified values plotted but they will be different for each instrument.

[53] Averaging the temperature field reduces the errors allowing a mean temperature change signal to be extracted. It is important to bear in mind however that when studying

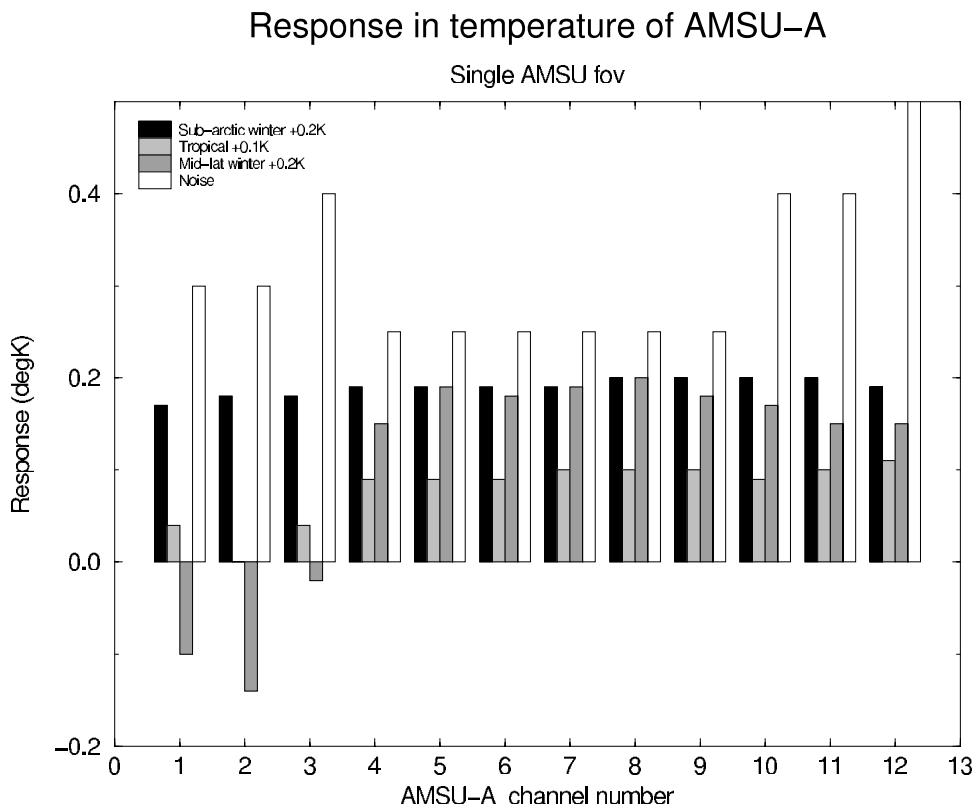

Figure 12. Response of AMSU-A channels to perturbations in temperature of the same order of magnitude as the CO_2 signal.

temporal trends in the AMSU-A or IASI/AIRS data the assumption does have to be made that there are no drifts in absolute calibration between both instruments. Regular collocations with radiosondes and aircraft reports can help to quantify drifts to within 0.1 K. Collocations with other satellite instruments (e.g., HIRS on METOP) will also be valuable for quantifying drifts. The experience of the MSU and AMSU-A radiometers suggests the microwave radiometers once launched are very stable in terms of radiometric calibration. Infrared radiometers or interferometers are more prone to contamination of the optics and a subsequent change of sensitivity with time although to first order this drift should be accounted for with the on-board calibration.

[54] In summary the AMSU-A channels can be used as a constraint on the temperature assumed in the IASI CO_2 retrieval probably to a level of 0.1 K. This should allow changes in CO_2 concentration of about 1% to be confidently inferred from the infrared radiances using the AMSU to define the temperature profile. Similarly the Microwave Humidity Sounder (MHS) and Humidity Sounder Brazil (HSB) can also provide an independent measurement of the humidity profile using the 183 GHz water vapor absorption line. This is less critical as channels can be selected from the infrared spectrum, which are insensitive to the water vapor concentration.

6.3. GPS Radio-Occultations

[55] Another source of independent temperature measurements is the radio-occultation GPS (Global Positioning System) soundings, which are planned from METOP and other satellites. The advent of the GPS allows receivers placed on low Earth orbiting spacecraft to view the GPS satellite constellation through atmospheric limb paths and enables the refractive index profile of the atmosphere to be retrieved. The refractive index data can then be related to the temperature and humidity profile [*Healy and Eyre*, 2000]. The concept of combining this information with interferometer radiances for climate monitoring is discussed by *Goody et al.* [1998]. These data either used in the vicinity of an IASI or AIRS measurement or assimilated in a NWP model to improve the model temperature and humidity fields should be a useful additional data source to help remove uncertainties in the temperature and water vapor fields. These measurements are not subject to drifts due to calibration in contrast to radiometer measurements.

7. Summary and Conclusions

[56] Monitoring atmospheric CO_2 concentrations from currently planned advanced IR sounder observations is clearly a challenging problem and will need careful preprocessing of the radiances in order not to swamp the CO_2 signal with other effects (e.g., undetected cloud, errors in assumed temperature profile). For a CO_2 retrieval to be possible the radiances must not only be *sensitive* to CO_2 concentration changes but also *separable* from other factors that influence them. IASI channels sensitive to the CO_2 perturbation but only weakly sensitive to uncertainties in water vapor, ozone, minor constituents and surface characteristics can be identified in both the SW and LW parts of the infrared spectrum. For the 15 micron CO_2 band uncertainties in temperature, water vapor and ozone all

affect the same region of the spectrum as CO_2 making the choice of channels in this wavelength region not affected by either water vapor or ozone more difficult. In the 4.4 micron band only temperature affects the same region of the spectrum as CO_2 and to a lesser extent than at 15 micron. The instrument noise for IASI is higher relative to the signal at the shorter wavelengths but for AIRS the instrument noise is lower. Therefore there is a trade-off between sensitivity to CO_2 relative to the instrument noise and reducing the interference from other absorbing molecules. The SW and LW parts of the spectrum should be used simultaneously to optimise the CO_2 retrieval. For IASI and AIRS the uncertainties in the atmospheric temperature and humidity profile can be reduced by including the coincident AMSU-A and MHS/HSB sounder data in the assimilation or retrieval process. The lower instrument noise of AIRS in the SW band may offer a better capability for monitoring CO_2 than IASI despite its lower spectral resolution.

[57] On the basis of current IASI noise estimates the simulations suggest an averaging of retrieved CO_2 fields of 500×500 km^2 in space and 15 days in time would achieve an accuracy of less than 1% in total column CO_2 amount. The CO_2 concentration information is primarily in a deep layer from the middle to upper troposphere. This should allow a global scale study of atmospheric CO_2 sources and sinks as long as the changes are not confined to the boundary layer. Ground measurements could provide absolute calibration, the satellite data giving the space and time gradients. Synoptic scale variations are more difficult since the required temporal resolution should be less than one day and although in this case the required accuracy is only 10 to 15 ppmv, the uncertainties in atmospheric temperature cannot be distinguished from the CO_2 changes.

[58] An information content study carried out shows that for AIRS radiances the SW CO_2 channels are more important for tropical profiles whereas for arctic profiles the LW CO_2 channels have more information. A set of 40–50 channels is required to extract most of the tropospheric CO_2 information for all atmospheric conditions.

[59] Variational data assimilation system (e.g., 4D-Var as described by *Klinker et al.*, 2000), which includes CO_2 as a variable in the model atmospheric state vector offers an interesting opportunity to infer the 3 dimensional global distribution of CO_2 from these sounders. The model background fields of temperature, water vapor and other minor constituents, including CO_2, are provided from a short range forecast from an analysis of the initial atmospheric state. This analysis has simultaneously assimilated all the observations available both direct (e.g., radiosonde profiles, aircraft reports) and indirect (e.g., radiances) to define the 3-dimensional state of the atmosphere at a given time. This assimilation process results in a reasonably accurate estimate of the initial atmospheric state compared with say a first guess climatological profile. Selected channels of the advanced sounder radiances, away from interfering species, would be assimilated along with all the other observations, taking into account their respective errors, using a fast radiative transfer model and its gradient as described by *Engelen et al.* [2001]. Forecast error covariances for carbon dioxide concentration will need to be estimated in order to distribute the inferred CO_2 perturbations to where the concentrations have their largest uncertainties in the model space. Care will need to be taken to estimate these errors as they strongly influence the analysed CO_2 fields. The microwave sounder radiances and GPS measurements will be assimilated simultaneously with the infrared radiances to help constrain the temperature and humidity profiles. Within the variational assimilation framework, as for other approaches used to infer global CO_2 concentrations, model biases (e.g., temperature, water vapor concentration) and observation biases (e.g., instrument calibration, radiative transfer model) have to be taken into account. Also the sources and sinks of CO_2 have to be adequately modelled.

[60] Alternatively stand-alone retrievals of CO_2 concentration and temperature profiles based on for example nonlinear neural networks trained on a diverse CO_2 profile data set could also be developed to provide an NWP independent data set for climate studies. This is proposed as part of the European COCO project to measure CO_2 from space by exploiting planned missions from 2001–2004.

[61] Finally clear sky IMG spectra, collocated with accurate temperature and moisture profiles, surface temperatures and emissivities have been processed to show their capability to study the ratio of $^{13}CO_2$ to $^{12}CO_2$, which could provide an indication of the nature of the CO_2 sources and sinks. This capability is probably beyond the limits of the advanced IR instruments now planned for launch on operational meteorological platforms.

[62] Future work to better assess how advanced infrared sounder data can provide information on CO_2 concentration should accomplish the following:

1. Assess whether our current knowledge of the spectroscopic parameters (e.g., line strengths, widths, coupling coefficients) is adequate for all CO_2 isotopes and identify regions of the spectrum where the spectroscopy is well understood and documented.
2. Determine the number of pixels to be averaged in space and time as a function of the required CO_2 accuracy and more accurate estimates of instrument noise.
3. Create a data set of CO_2 concentration profiles representative of natural and human-induced variability.
4. Upgrade fast radiative transfer models (e.g., RTIASI, *Matricardi and Saunders* [1999] or the neural network model, Advanced Rapid Radiance Reconstruction Network (A3R-N) by *Montandon et al.* [2002]) to include CO_2 as a variable gas and to compute the Jacobians with respect to CO_2.

[63] **Acknowledgments.** This work was carried out under a EUMETSAT funded contract (98/310). F. Cayla provided the latest IASI noise figures for the calculations presented here and L. Strow the AIRS instrument characteristics. We thank P. Ciais for helpful discussions. The IMG level 1c data was provided by IMGDIS/ERSDAC for which the authors are grateful. The authors also acknowledge useful comments from two anonymous reviewers who helped to improve the initial drafts.

References

Amato, U., V. Cuomo, I. De Feis, F. Romano, C. Serio, and H. Kobayashi, Inverting for geophysical parameters from IMG radiances, *IEEE Trans. Geosci. Remote Sens.*, *37*, 1620–1632, 1999.

Aumann, H. H., and R. J. Pagano, Atmospheric infrared sounder on Earth observing system, *Optical Eng.*, *33*, 776–784, 1994.

Bousquet, P., Optimisation des flux nets de CO_2: Assimilation des mesures atmosphériques en CO_2 et en $^{13}CO_2$ dans un modèle de transport tridimensionnel, Thèse Paris 6, 1997a.

Bousquet, P., A. Gaudry, P. Ciais, V. Kazan, P. Monfray, P. G. Simmons, S. G. Jennings, and T. C. O'Connors, Atmospheric CO_2 concentration variations recorded at Mace Head, Ireland, from 1992 to 1994, *Phys. Chem. Earth*, *21*, 477–481, 1997b.

Bousquet, P., P. Peylin, P. Ciais, M. Ramonet, and P. Monfray, Inverse modelling of annual atmospheric CO_2 sources and sinks, 1, Method and control inversion, *J. Geophys. Res.*, *104*, 26,161–26,178, 1999.

Buchwitz, M. V., V. Rozanov, and J. P. Burrows, A near-infrared optimized DOAS method for the fast retrieval of atmospheric CH_4, CO, CO_2, H_2O and N_2O total column amounts from Schiamachy ENVISAT-1 nadir radiances, *J. Geophys. Res.*, *105*, 15,231–15,246, 2000.

Cayla, F., Simulation of IASI spectra, CNES document IA-TN-0000-5627-CNE (Centre National d'Etudes Spatiales, Toulouse), 1996.

Ciais, P., P. P. Tans, M. Trolier, J. W. White, and R. Francey, A large northern hemisphere terrestrial CO_2 sink indicated by the $^{13}C/^{12}C$ ratio of atmospheric CO_2, *Science*, *269*, 1098–1102, 1995.

Chédin, A., N. A. Scott, R. Saunders, M. Matricardi, J. Etcheto, and C. Clerbaux, IASI capability to monitor CO_2, Final Report, EUMETSAT Contract N° 98/310, 1999.

Chédin, A., S. Serrar, R. Armante, N. A. Scott, and A. Hollingsworth, Signatures of Annual and Seasonal Variations of CO_2 and Other Greenhouse Gases from Comparisons between NOAA TOVS Observations and Radiation Model Simulations, *J. Clim.*, *15*, 95–116, 2002a.

Chédin, A., A. Hollingsworth, N. A. Scott, S. Serrar, C. Crevoisier, and R. Armante, Annual and seasonal variations of atmospheric CO_2, N_2O and CO concentrations retrieved from NOAA/TOVS satellite observations, *Geophys. Res. Lett.*, *29*, doi:10.1029/2001GL014082, 2002b.

Clerbaux, C., J. Hadji-Lazaro, S. Payan, C. Camy-Peyret, and G. Mégie, Retrieval of CO columns from IMG/ADEOS spectra, *IEEE Trans. Geosci. Remote Sens.*, *37*, 1657–1662, 1999.

Conway, T. J., P. P. Tans, L. S. Waterman, K. W. Thoning, D. R. Kitzis, K. A. Masarie, and N. Zhang, Evidence for interannual variability of the carbon cycle from the National Oceanic and Atmospheric Administration/Climate Monitoring and Diagnostic Laboratory Global Air Sampling, *J. Geophys. Res.*, *99*, 22,831–22,855, 1994.

Edwards, D. P., GENLN2: A general line-by-line atmospheric transmittance and radiance model, NCAR Technical Note NCAR/TN-367 + STR, Natl. Cent. for Atmos. Res., Boulder, Colo., 1992.

Engardt, M., K. Holmen, and J. Heintzenberg, Short-term variations in atmospheric CO_2 at Ny-Alesund, Spitsbergen during spring and summer, *Tellus*, *48B*, 33–43, 1996.

Engelen, R. J., A. Scott Denning, H. R. Gurney, and G. L. Stephens, Global Observations of the carbon budget, I, Expected satellite capabilities for emission spectroscopy in the EOS and NPOESS eras, *J. Geophys. Res.*, *106*, 20,055–20,068, 2001.

Enting, I. G., and G. I. Pierman, Average global distribution of CO_2, in *The Global Carbon Cycle*, edited by M. Heimenn, pp. 31–64, NATO ASI Series, Spinger-Verlag, New York, 1993.

Francey, R. J., F. J. Robbins, C. E. Allison, and N. G. Richards, The CSIRO global survey of CO_2 stable isotopes, Baseline 1988, edited by A. C. T. Canberra, Bur. of Meteorol., W.S.R., Australia, 1990.

Garand, L., et al., Radiance and Jacobian intercomparison of radiative transfer models applied to HIRS and AMSU channels, *J. Geophys. Res.*, *106*, 24,017–24,031, 2001.

Gaudry, A., P. Monfray, G. Polian, and G. Lambert, Radar-calibrated emissions of CO_2 from South Africa, *Tellus*, *42B*, 9–19, 1990.

GLOBALVIEW-CO2: Cooperative Atmospheric Data Integration Project - Carbon Dioxide [CD-ROM], NOAA CMDL, Boulder, Colo., 2000. [Also available on Internet via anonymous FTP to ftp.cmdl.noaa.gov, Path: ccg/co2/GLOBALVIEW]

Goody, R., J. Anderson, and G. North, Testing climate models: An approach, *Bull. Am. Meteorol. Soc.*, *79*, 2541–2549, 1998.

Hadji-Lazaro, J., C. Clerbaux, and S. Thiria, An inversion algorithm using neural networks to retrieve atmospheric CO concentrations from high-resolution nadir radiances, *J. Geophys. Res.*, *104*, 23,841–23,854, 1999.

Hadji-Lazaro, J., C. Clerbaux, P. Couvert, P. Chazette, and C. Boonne, Cloud filter for CO retrieval from IMG infrared spectra using ECMWF temperatures and POLDER cloud data, *Geophys. Res. Lett.*, *28*, 2397–2400, 2001.

Healy, S. B., and J. R. Eyre, Retrieving temperature, water vapor and surface pressure information from refractive-index profiles derived by radio occultation: A simulation study, *Quart. J. Roy. Meteorol. Soc.*, *126*, 1661, 2000.

Heimann, M., and C. D. Keeling, A three-dimensional model of atmospheric CO_2 transport based on observed winds, 2, Model description and simulated tracer experiments, aspects of climate variability in the Pacific and Western Americas, *Geophys. Monograph Ser.*, vol. 55, edited by D. H. Peterson, pp. 237–275, AGU, Washington, D. C., 1989.

Heimann, M., The Global Atmospheric Tracer Model TM2, Rapport n°10, Max-Planck Institute fur Meteorologie, Hamburg, 1995.

Hood, E. M., L. Merlivat, and T. Johannessen, Variations of fCO_2 and air-sea flux of CO_2 in the Greenland Sea gyre using high-frequency time-series data from CARIOCA drift-buoys, *J. Geophys. Res.*, *104*, 20,571–20,583, 1999.

Hood, E. M., and L. Merlivat, Annual to interannual variations of fCO_2 in the northwestern Mediterranean sea: Results from hourly measurements made by CARIOCA buoys, 1995–1997, *J. Mar. Res.*, *59*, 113–131, 2001.

Jacquinet-Husson, N., et al., The 1997 spectroscopic GEISA data bank, *J. Quant. Spectrosc. Radiat. Transfer*, *62*, 205–254, 1999.

Keeling, C. D., The concentration and isotopic abundances of carbon dioxide in the atmosphere, *Tellus*, *12*, 200–203, 1960.

Keeling, C. D., R. B. Bacastow, A. F. Carter, S. C. Piper, T. P. Whorf, M. Heimann, W. G. Mook, and H. A. Roeloffzen, A three-dimensional model of atmospheric CO_2 transport based on observed winds, 1, Analysis of observational data, aspects of cimate variability in the Pacific and Western Americas, *Geophys. Monograph Ser.*, vol. 55, edited by D. H. Peterson, pp. 165–236, AGU, Washington, D. C., 1989.

Klinker, E., F. Rabier, G. Kelly, and J.-F. Mahfouf, The ECMWF operational implementation of four-dimensional variational assimilation, III, Experimental results and diagnostics with operational configuration, *Quart. J. Roy. Meteorol. Soc.*, *126*, 1191–1216, 2000.

Kobayashi, H., A. Shimota, K. Kondo, E. Okumura, Y. Kameda, H. Shimoda, and T. Ogawa, Development and evaluation of the interferometric monitor for greenhouse gases: A high-throughput Fourier-transform infrared radiometer for nadir Earth observations, *Appl. Opt.*, *38*, 6801–6807, 1999a.

Kobayashi, H., A. Shimota, C. Yoshigahara, I. Yoshida, Y. Uehara, and K. Kondo, Satellite-borne high-resolution FTIR for lower atmosphere sounding and its evaluation, *IEEE Trans. Geosci. Remote Sens.*, *37*, 1496–1507, 1999b.

Lubrano, A. M., C. Serio, S. A. Clough, and H. Kobayashi, Simultaneous inversion for temperature and water vapor from IMG radiances, *Geophys. Res. Lett.*, *27*, 2533–2536, 2000.

Masarie, K. A., and P. P. Tans, Extension and integration of atmospheric carbon dioxide data into a globally consistent measurement record, *J. Geophys.*, 11,593–11,610, 1995.

Masuda, K., T. Takashima, and T. Takayama, Emissivity of pure sea waters for the model sea surface in the infrared window regions, *Remote Sens. Environ.*, *24*, 313–329, 1988.

Matricardi, M., and R. W. Saunders, A fast radiative transfer model for simulation of IASI radiances, *Appl. Opt.*, *38*, 5679–5691, 1999.

Nakazawa, T., K. Miyashita, S. Aoki, and M. Tanaka, Temporal and spatial variations of upper tropospheric and lower stratospheric carbon dioxide, *Tellus*, *43B*, 106–117, 1991.

Park, J. H., Atmospheric CO_2 monitoring from space, *Appl. Opt.*, *36*, 2701–2712, 1997.

Peylin, P., B. Picard, P. Bousquet, F. M. Breon, and P. Ciais, Potential of column integrated CO_2 fluxes using inverse methods, 4th GEWEX Symposium, Paris, France, 2001.

Prunet, P., J.-N. Thépaut, and V. Cassé, The information content of clear sky IASI radiances and their potential for numerical weather prediction, *Q. J. R. Meteorol. Soc.*, *124*, 211–242, 1998.

Rabier, F., N. Fourrié, D. Chafaï, and P. Prunet, Channel selection methods for infrared atmospheric sounding interferometers radiances, *Q. J. R. Meteorol. Soc.*, *128*, 1011–1028, 2002.

Ramonet, M., Variabilité du CO_2 atmosphérique en régions australes: Comparaison modèle/mesures, Thèse Paris 6, 1994.

Rayner, P. J., I. G. Enting, R. J. Francey, and R. L. Langenfelds, Reconstructing the recent carbon cycle from atmospheric CO_2, $\delta^{13}C$ and O_2/N_2 observations, *Tellus*, *51B*, 213–232, 1999.

Rayner, P. J., and D. M. O'Brien, The utility of remotely sensed CO_2 concentration data in surface source inversions, *Geophys. Res. Lett.*, *28*, 175–178, 2001.

Rodgers, C. D., Information content and optimisation of high spectral resolution measurements, Optical Spectroscopic Techniques and Instrumentation for Atmospheric and Space Research, II, *SPIE*, *2830*, 136–147, 1996.

Rothman, L. S., et al., The HITRAN molecular spectroscopic database and HAWKS (HITRAN atmospheric workstation): 1996 edition, *J. Quant. Spectrosc. Radiat. Trans.*, *60*, 665–710, 1998.

Saunders, R. W., M. Matricardi, and P. Brunel, An improved fast radiative transfer model for assimilation of satellite radiance observations, *Q. J. R. Meteorol. Soc.*, *125*, 1407–1425, 1999.

Schimel, D., et al., Radiative Forcing of Climate Change, in *Climate Change 1995, The Science of Climate Change*, edited by J. T. Houghton et al., pp. 69–131, Cambridge Univ. Press, New York, 1995.

Scott, N. A., A direct method of computation of the transmission function of an inhomogeneous gaseous medium: Description of the method and influence of various factors, *J. Quant. Spectrosc. Radiat. Trans.*, *14*, 691–707, 1974.

Scott, N. A., and A. Chedin, A fast line-by-line method for atmospheric absorption computations: "The Automatized Atmospheric Absorption Atlas", *J. Appl. Meteorol.*, *20*, 556–564, 1981.

Snyder, W. C., Z. Wan, Y. Zhang, and Y.-Z. Feng, Classification-based emissivity for land surface temperature measurement from space, *Int. J. Remote Sens.*, *19*, 2753–2774, 1988.

Spencer, R. W., and J. R. Christy, Precision lower stratospheric temperature monitoring with the MSU: Validation and results 1979–1991, *J. Clim.*, *6*, 1194–1204, 1993.

Strow, L. L., D. C. Tobin, and S. E. Hannon, A compilation of first-order line-mixing coefficients for CO_2 Q-branches, *J. Quant. Spectrosc. Radiat. Trans.*, *52*, 281, 1994.

Tans, P. P., I. Y. Fung, and T. Takahashi, Observational constraints on the global atmospheric CO_2 budget, *Science*, *247*, 1431–1438, 1990.

Tournier, B., R. Armante, and N. A. Scott, STRANSAC-93 et 4A-93: Developpement et validation des nouvelles version des codes de transport radiatif pour application projet IASI, *Internal Rep. LMD*, *No. 201*, LMD/CNRS, Ecole Polytechnique, PALAISEAU, France, 1995.

Trolier, M., J. W. C. White, P. P. Tans, K. A. Masarie, and P. A. Gemery, Monitoring the isotopic composition of atmospheric CO_2: Measurements from the NOAA global air sampling network, *J. Geophys. Res.*, *101*, 25,897–25,916, 1996.

Turquety, S. J., J. Hadji-Lazaro, and C. Clerbaux. Retrieval of ozone from infrared IASI measurements, in *Remote Sensing of Clouds and the Atmosphere VI*, edited by K. Schaefer et al., pp. 106–115, *Proc. SPIE*, *4539*, 2002.

R. Armante, A. Chédin, C. Crevoisier, and N. Scott, Laboratoire de Météorologie Dynamique, École Polytechnique, 91128 Palaiseau, France. (armante@lmd.polytechnique.fr; chedin@lmd.polytechnique.fr; crevoisier@lmd.polytechnique.fr; nas@lmd.polytechnique.fr)

C. Clerbaux, Service d'Aéronomie, Université de Paris 6, Paris, France. (catherine.clerbaux@aero.jussieu.fr)

J. Etcheto, Laboratoire d'Océanographie Dynamique et de Climatologie, Université Pierre et Marie Curie, Paris, France.

A. Hollingsworth, M. Matricardi, and R. W. Saunders, ECMWF, Shinfield Park, Reading RG2 9AX, U.K. (dia@ecmwf.int; stm@ecmwf.int; roger.saunders@metoffice.com)